

Analysis of the shear layer instability process of a laminar separation bubble by means of Dynamic Mode Decomposition technique

V. Bologna^{1*}, M. Dellacasagrande¹, P. Przytarski¹, D. Lengani¹ and D. Simoni¹

1: Department of Mechanical, Energy, Management and Transport Engineering (DIME)
University of Genova, 16145, Italy

* Corresponding authors: virginia.bologna@edu.unige.it

Abstract

This study examines the shear layer instability of a laminar separation bubble (LSB) under varying flow conditions using Dynamic Mode Decomposition (DMD). The analysis decomposes the flow into DMD modes, revealing frequencies and growth rates associated with shear layer disturbances that lead to energetic vortex shedding. The investigation focuses on changes in the stability of the separated boundary layer (BL) at different Reynolds numbers, ranging from 10,000 to 65,000. The data, obtained from Particle Image Velocimetry (PIV) measurements in a controlled wind tunnel environment, highlight the onset and evolution of shear layer instabilities characterized by variations in wavelength and frequency. The results demonstrate that DMD provides a detailed characterization of the spatial and temporal growth of disturbances, offering insight into the transition from stable to unstable states in LSBs as external flow conditions change.

Keyword: *Laminar Separation Bubble, Dynamic Mode Decomposition, transient dynamics, shear layer instability*

1. Introduction

Boundary layer (BL) separation can occur in the presence of an adverse pressure gradient (APG), moderate Reynolds numbers (Re), and low free-stream turbulence levels (Tu). The detachment of the boundary layer from a solid surface can occur for both continuous and fixed pressure gradients [15, 14], high positive incidence angles [25], or geometric discontinuities [9]. When the shear layer transitions to turbulence and reattaches to the wall, a laminar separation bubble (LSB) forms, characterized by a region of reversed flow near the wall [26]. The transition of an LSB is typically driven by the inviscid Kelvin-Helmholtz (K-H) instability [11]. The growth of fluctuations leads to shear layer roll-up and the formation of spanwise vortices, causing momentum transfer towards the wall [20] and high turbulence production [24]. The main parameters affecting both the statistics and the dynamics of an LSB are the Reynolds number, the free-stream turbulence intensity, and the pressure gradient [7]. Reynolds number and turbulence level variations can cause marked changes in the LSB dimensions, causing significant modifications in the surface pressure distribution, even upstream of the separation position [19, 28, 10]. Depending on the turbulence level and Reynolds number, streaky structures (typical of bypass transition) may propagate within the separated shear layer without necessarily suppressing the LSB [17, 24]. K-H rolls may be perturbed by these elongated structures, which accelerate their disruption [24]. Studies, such as [29] and [12], have explored the response of LSBs to varying Reynolds numbers and free-stream turbulence, revealing that streaks can induce three-dimensional shear layer roll-up.

The stability of LSBs has been widely studied using linear stability theory (LST) [22, 13, 8, 4, 1, 27]. LST accurately predicts unstable wavelengths characterizing K-H instability under various turbulence levels. Data-driven techniques like Spectral Proper Orthogonal Decomposition (SPOD) and Dynamic Mode Decomposition (DMD, [23, 16]) have also been employed to identify unstable boundary layer modes from experimental and numerical data [18, 31, 30, 33, 21, 32]. For instance, [31] used SPOD to study low-frequency breathing motions of a turbulent separation bubble, while [32] applied DMD to high-fidelity numerical data,

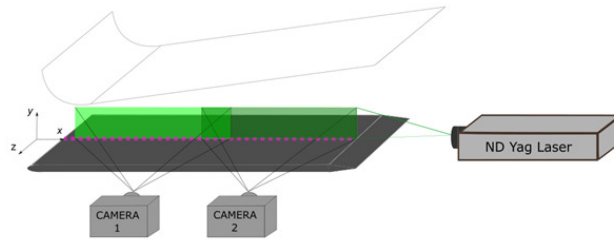


Fig. 1: Test section and PIV instrumentation layout. Only the top wall is shown, as the bottom one is set symmetrically. Green boxes highlight the PIV measurement domain.

capturing both low- and high-frequency modes. Recent modifications in DMD procedures have enabled the characterization of transient behaviors in LSBs [30].

This work investigates the shear layer instability of a flat plate laminar separation bubble by means of the application of a DMD based procedure on Particle Image Velocimetry (PIV) data. DMD decomposes the flow into modes with corresponding frequencies and growth rates, illustrating how shear layer disturbances evolve spatially during a transient process, leading to the formation of Kelvin-Helmholtz vortices. Spatial DMD was applied under two different conditions — representative of a long and a short bubble state — both characterized by the same adverse pressure gradient and free-stream turbulence intensity, to examine changes in shear layer stability with varying Reynolds numbers.

2. Experimental setup

The data used in this study comes from an extensive experimental database of flat plate laminar separation bubbles, covering both short and long types, across 72 combinations of flow conditions (Re , APG and Tu). Experiments were conducted in a low-speed, open-loop wind tunnel at the Aerodynamic and Turbomachinery Laboratory of the University of Genova. Measurements of 2D flow velocity fields were obtained in the mid-span section of the plate using a Particle Image Velocimetry (PIV) instrumentation (see Fig. 1). The measuring domain spanned from approximately $x/L = 0.2$ to $x/L = 1$ streamwise and $y/L = 0.07$ normal to the wall directions, respectively ($L=300$ mm is the plate length). Velocity maps were generated using a magnification factor of 0.16 and interrogation areas of 16×16 pixels, with a 50% overlap, achieving a spatial resolution of 0.41 mm. Data pre-processing included adaptive cross-correlation, peak validation, Gaussian fitting for sub-pixel accuracy, and uncertainty estimation using the peak-ratio method by [5]. For each set of flow conditions, 6000 PIV snapshots were captured at 1 kHz to achieve convergence on the time-mean flow field and resolve vortex shedding frequencies. The study focuses on transient LSB dynamics under two time-varying Reynolds number conditions ($Re = 17,000$ and $Re = 62,000$), at a fixed free-stream turbulence intensity ($Tu=3.5\%$) and adverse pressure gradient. The adverse pressure gradient was set using adjustable end-walls at a 12° opening angle.

3. DMD based procedure

To define a proper state space for characterizing the statistical and dynamic response of a laminar separation bubble to changes in external flow parameters, all 72 flow cases in the original database were analyzed using Proper Orthogonal Decomposition (POD) [2] [3]. In this work, only the POD coefficients corresponding to the examined conditions were considered, specifically those identified as Kelvin-Helmholtz modes, as discussed in section 4. The analysis of the acquired snapshots in the state space constituted by the POD coefficients describing the vortex shedding dynamics further highlighted the time-varying dynamics of the shear layer instability process. This observation was supported by visual inspection of PIV snapshots showing the evolution of the LSB over time, revealing changes in shear layer instability caused by slight variations in free-stream velocity, leading to substantial alterations in the intensity of the vortex train developing in the rear part of the bubble. To investigate this transient process in more detail, a spatial DMD analysis was conducted for temporal and spatial sub-blocks, enabling the study of the growth rate of the Kelvin-Helmholtz modes in both space and time. This analysis confirmed the unstable nature of the mode at instances where marked fluctuations in the POD coefficients related to vortex shedding were observed.

Figure 2 shows a schematic representation of the spatial block-wise DMD method used in the present work.

Analysis of the shear layer instability process of a laminar separation bubble by means of Dynamic Mode Decomposition technique

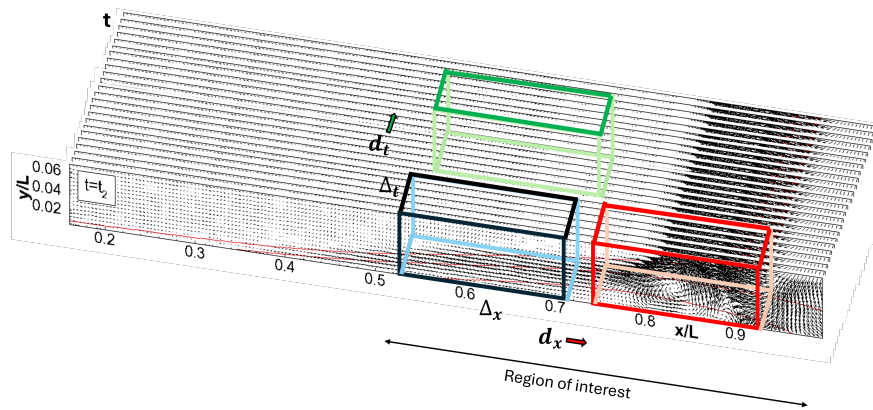


Fig. 2: Schematic of the spatial block-wise DMD procedure. The blue box represents a block in the streamwise direction and time, while red and green boxes indicate spatial and temporal shifting directions, respectively.

DMD was applied from the separation position to the end of the plate surface ($x/L = 1$). Spatial Δ_x and temporal Δ_t extension of sub-blocks (see blue block in Fig. 2) were chosen based on the characteristic wavelength and frequency of the K-H modes, as provided by the POD analysis. More specifically, for $Re = 17,000$, $\Delta_t = 0.2$ s and $\Delta_x = 50$ mm, while for $Re = 62,000$, $\Delta_t = 0.035$ s and $\Delta_x = 28$ mm. DMD modes were recorded for each spatio-temporal position. According to the current method, the complex DMD eigenvalues λ , retain the spatial growth or decay rate (σ , real part) of streamwise wavelengths (λ_{wave} , imaginary part) [23, 16]. The spatial DMD algorithm was repeated spanning the domain with a spatial increment of δ_x equal to the spatial resolution of the PIV measurements (see red block in Fig. 2). This approach allowed the analysis of the evolution of spatio-temporal coherent structures (represented by the DMD modes) along the streamwise development of the LSB, by examining the evolution of the corresponding growth rates and wavelengths along the flow direction. The DMD was also repeated by shifting the block by one snapshot ($\delta_t = 0.001$ s) along the time axis (see green block in Fig. 2), enabling the dynamic characterization of the most unstable modes. The DMD modes obtained for each block were then ordered based on their characteristic wavelength. Then, the evolution of the growth rates and wavelengths was analyzed by considering the same mode across different blocks, ensuring a consistent dynamic mode basis for comparison. This specifically allowed observation of the spatio-temporal evolution of a specific structure (described by the DMD mode) characterized, on average, by a particular wavelength, such as that of the K-H rolls of the two analyzed conditions.

4. Results

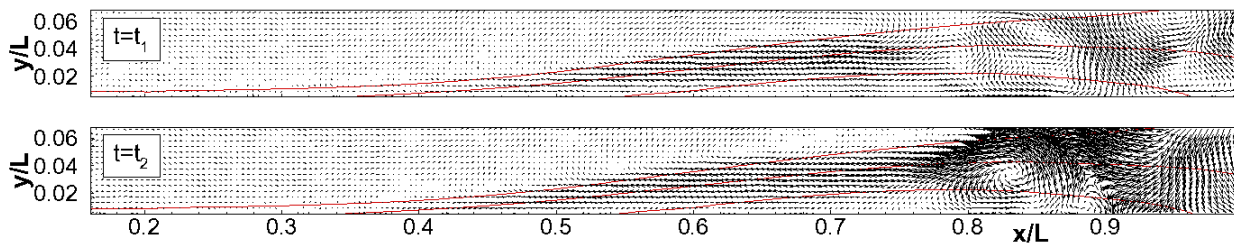


Fig. 3: Velocity vector maps for $Re = 17,000$. Top: unperturbed shear layer at $t = t_1$; Bottom: strong vortex shedding at $t = t_2$ due to increased instabilities.

Figures 3 and 4 show the vector maps of instantaneous fluctuating velocity for $Re = 17,000$ and $Re = 62,000$, respectively. Figure 3 displays a long bubble configuration, while figure 4 shows a short bubble configuration (see [6] for further details). The top plots, labelled as $t = t_1$, do not show the occurrence of spanwise vortices in none of the cases. In contrast, the bottom plots, time $t = t_2$, show pronounced vortex shedding. The transition between different vortex shedding behaviors was observed throughout the entire

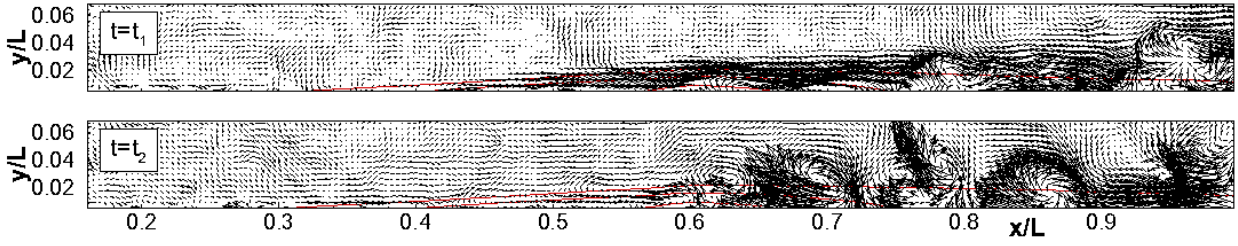


Fig. 4: Velocity vector maps for $Re = 62,000$. Top: unperturbed shear layer at $t = t_1$; Bottom: strong vortex shedding at $t = t_2$ due to increased instabilities.

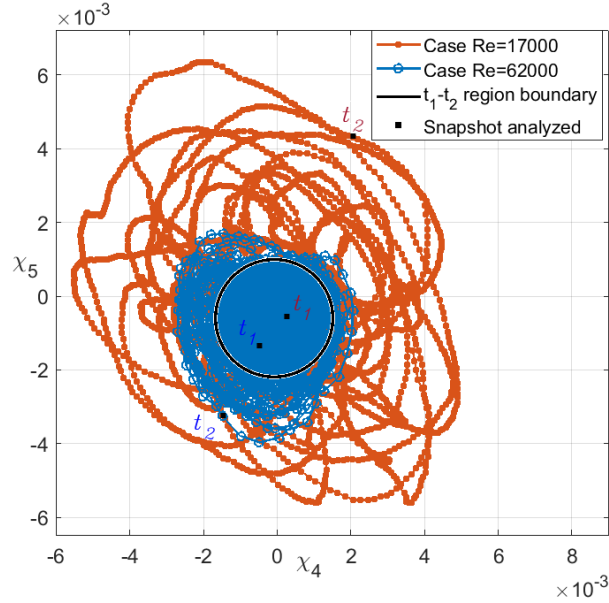


Fig. 5: POD reduced state-space characterized by coefficients related to K-H modes.

temporal evolution of the bubble, across all 6000 PIV snapshots. Time-marching spatial DMD analysis was used to provide a statistical characterization of the vortex shedding variation in both space and time.

To better highlight the temporal variation of the shedding process characteristics, the acquired flow states were examined in the POD space defined by the shedding-related coefficient χ_4 and χ_5 (Fig. 5). In case of steady shedding process, the chosen coefficients are known to lay on an accurately determined boundary of a circle. Instead, Fig. 5 shows that the POD coefficients alternatively collapse and expand in time, suggesting an unsteady behavior of the shedding phenomenon. Two distinct regions were identified in the present POD space by means of a Gaussian classifier characterized by a normal distribution with variance 2Σ (see black circle in Fig. 5). One region was seen to be characterized by low-frequency, low-amplitude fluctuations, and the other one by high-frequency, high-amplitude oscillations. The first is associated to the flow patterns observed in the time-instants labelled as t_1 in Figs. 3-4. The second one to time instants named as t_2 . The current DMD procedure was used to provide a detailed characterization of the shear layer instability in the different regions of the POD state space. More specifically, comparing data reported in Fig. 5 with the results of the DMD analysis will highlight changes in the stability characteristics driving the unsteady behavior of the shedding process.

Figure 6 presents contour plots of the growth rate σ of K-H modes over time t and along the streamwise direction x/L for the examined Re cases. A zoomed view is provided to observe the transition of the shedding phenomenon from steady to unsteady behavior. Indeed, the change of the growth rate from negative to positive values indicates the presence of shear layer instabilities and the formation of K-H rolls. For both the Re cases, a clear core of disturbances, characterized by peak growth rates, develops over time along the entire

Analysis of the shear layer instability process of a laminar separation bubble by means of Dynamic Mode Decomposition technique

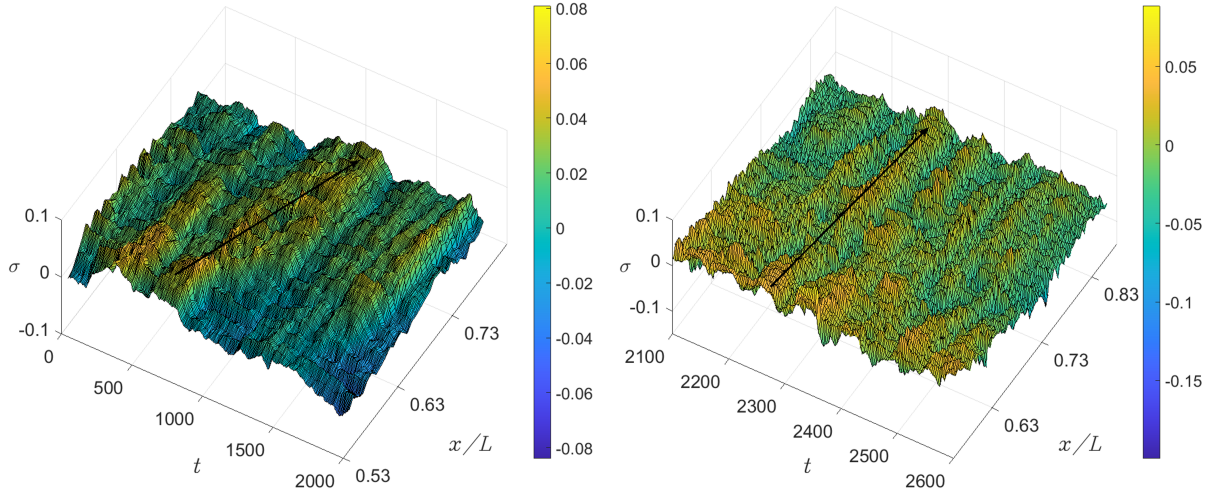


Fig. 6: Contour plots of the growth rate related to shear layer instability: $Re = 17,000$ (left) and $Re = 62,000$ (right).

bubble length (see black arrows in Fig. 6). These instabilities lead to unstable Kelvin-Helmholtz modes and energetic vortex shedding, as confirmed by the visual inspection of PIV snapshots.

To further reduce the data shown in Fig. 6, the conditional average value of the growth rate of the K-H wavelength was computed for regions of high and low amplitude of the K-H related coefficients (Fig. 5). Results are shown in figure 7. For $Re = 17,000$, the growth rate within the zone of low amplitude coefficient (t_1 zone), highlighted in Fig. 5, is generally negative, transitioning to positive values towards the rear part of the bubble, suggesting the onset of vortex shedding around $x/L = 0.7$ for a long bubble. Outside of this region (t_2 zone), the growth rate remains consistently positive, indicating an unstable shear layer with disturbances growing up to the bubble's maximum height. At $Re = 62,000$, the growth rate is typically

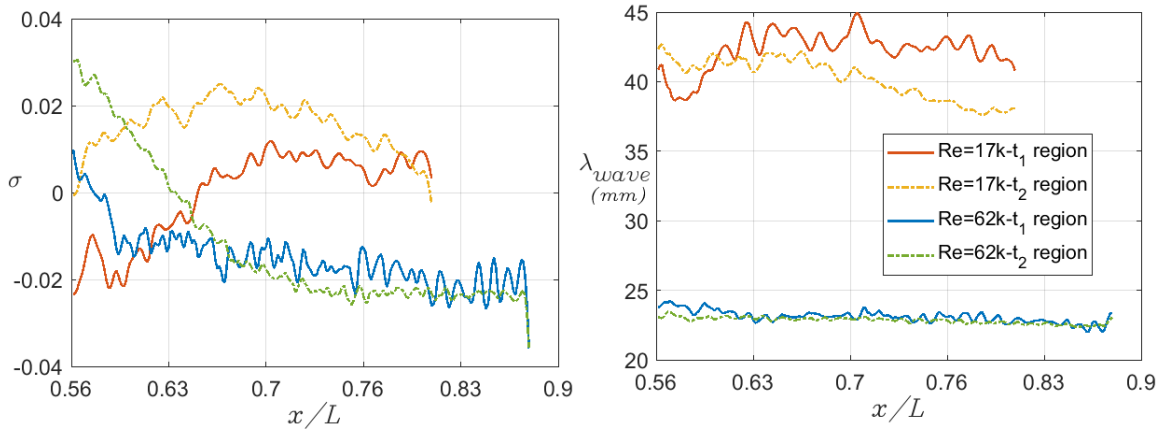


Fig. 7: Average growth rate and wavelength trends along the streamwise direction for $Re = 17,000$ (left) and $Re = 62,000$ (right).

negative throughout the bubble's development inside the t_1 region, characterized by steady behavior of the shedding phenomenon, indicating a stable shear layer. Outside of it, the growth rate is high and positive in the front part of the bubble, then decreases as the vortex structures break down. The shorter wavelengths for the higher Re case reflect faster dynamics (i.e. higher growth rates) in the shorter bubble configuration. The right plot, showing the time-average wavelength for different regions of the POD sub-space defined in Fig. 5, shows consistency of the detected dynamics, with the same unstable wavelength highlighted for a fixed Reynolds number.

5. Conclusion

The present research demonstrated that shear layer instability in laminar separation bubbles can be effectively characterized using Dynamic Mode Decomposition technique. Indeed, the application of block-wise spatial DMD allowed for the characterization of changes in the stability characteristics of the separated boundary layer, due to variations in external flow velocity, that drive the transition of the shedding process from steady to unsteady behavior. The temporal and spatial analysis of the growth rates associated with the K-H modes made it possible to distinguish between time intervals where the dominant K-H modes are stable and transient periods where disturbance growth is observed due to changes in the flow Reynolds number.

References

- [1] S Mohamed Aniffa et al. “Characteristics of geometry-and pressure-induced laminar separation bubbles at an enhanced level of free-stream turbulence”. In: *Journal of Fluid Mechanics* 957 (2023), A19.
- [2] Gal Berkooz, Philip Holmes, and John L Lumley. “The proper orthogonal decomposition in the analysis of turbulent flows”. In: *Annual review of fluid mechanics* 25.1 (1993), pp. 539–575.
- [3] Virginia Bologna et al. “Compressed Representation of Separation Bubbles from a Vast Database”. In: *Available at SSRN 4836229* ().
- [4] David Borgmann et al. “Investigation of laminar separation bubbles using experiments, theory and DNS”. In: *AIAA Aviation 2021 Forum*. 2021, p. 2898.
- [5] John J Charonko and Pavlos P Vlachos. “Estimation of uncertainty bounds for individual particle image velocimetry measurements from cross-correlation peak ratio”. In: *Measurement Science and Technology* 24.6 (2013), p. 065301.
- [6] Matteo Dellacasagrande et al. “An Experimental Database for the Analysis of Bursting of a Laminar Separation Bubble”. In: *International Journal of Turbomachinery, Propulsion and Power* 9.1 (2024), p. 3.
- [7] Matteo Dellacasagrande et al. “Response of a flat plate laminar separation bubble to Reynolds number, free-stream turbulence and adverse pressure gradient variation”. In: *Experiments in Fluids* 61.6 (2020).
- [8] Sourabh S Diwan and ON Ramesh. “Relevance of local parallel theory to the linear stability of laminar separation bubbles”. In: *Journal of fluid mechanics* 698 (2012), pp. 468–478.
- [9] Xingjun Fang and Mark F Tachie. “Spatio-temporal dynamics of flow separation induced by a forward-facing step submerged in a thick turbulent boundary layer”. In: *Journal of Fluid Mechanics* 892 (2020), A40.
- [10] M Gaster. “The structure and behaviour of laminar separation bubbles”. In: *Technical report, Aeronautical Research Council* (1967).
- [11] Shirzad Hosseinverdi and Hermann F Fasel. “Numerical investigation of laminar–turbulent transition in laminar separation bubbles: the effect of free-stream turbulence”. In: *Journal of Fluid Mechanics* 858 (2019), pp. 714–759.
- [12] M. S. Istvan, J. W. Kurelek, and S. Yarusevych. “Turbulence Intensity Effects on Laminar Separation Bubbles Formed over an Airfoil”. In: *AIAA Journal* 56.4 (2018), pp. 1335–1347.
- [13] L. Jones, R. Sandberg, and N. Sandham. “Direct Numerical Simulations of Forced and Unforced Separation Bubbles on an Airfoil at Incidence”. In: *J. Fluid Mech.* 602 (2008), pp. 175–207.
- [14] Ravi Kumar and S Sarkar. “Features of laminar separation bubble subjected to varying adverse pressure gradients”. In: *Physics of Fluids* 35.12 (2023).
- [15] John W Kurelek et al. “Three-dimensional development of coherent structures in a two-dimensional laminar separation bubble”. In: *AIAA Journal* 59.2 (2021), pp. 493–505.
- [16] J. N. Kutz et al. *Dynamic mode decomposition: data-driven modeling of complex systems*. Vol. 149. SIAM, 2016.
- [17] S. Lardeau, M. Leschziner, and T. Zaki. “Large eddy simulation of transitional separated flow over a flat plate and a compressor blade”. In: *Flow Turbul. and Combust.* 88 (2012), pp. 919–944.
- [18] Davide Lengani et al. “Experimental study of free-stream turbulence induced transition in an adverse pressure gradient”. In: *Experimental Thermal and Fluid Science* 84 (2017), pp. 18–27.

Analysis of the shear layer instability process of a laminar separation bubble by means of Dynamic Mode Decomposition technique

- [19] O. Marxen and D. S. Henningson. “The Effect of Small-Amplitude Convective Disturbances on the Size and Bursting of a Laminar Separation Bubble”. In: *J. Fluid Mech.* 671 (2011), pp. 1–33.
- [20] O. Marxen, M. Lang, and U. Rist. “Vortex formation and vortex breakup in a laminar separation bubble”. In: *J Fluid Mech* 728 (2013), pp. 58–90.
- [21] Stephan Priebe et al. “Low-frequency dynamics in a shock-induced separated flow”. In: *Journal of Fluid Mechanics* 807 (2016), pp. 441–477.
- [22] Daniel Rodriguez and Vassilis Theofilis. “Structural changes of laminar separation bubbles induced by global linear instability”. In: *Journal of Fluid Mechanics* 655 (2010), pp. 280–305.
- [23] Peter J Schmid et al. “Applications of the dynamic mode decomposition”. In: *Theoretical and computational fluid dynamics* 25 (2011), pp. 249–259.
- [24] Aditi Sengupta and Paul Tucker. “Effects of forced frequency oscillations and free stream turbulence on the separation-induced transition in pressure gradient dominated flows”. In: *Physics of Fluids* 32.10 (2020).
- [25] JA Smith, Gabriele Pisetta, and Ignazio Maria Viola. “The scales of the leading-edge separation bubble”. In: *Physics of Fluids* 33.4 (2021).
- [26] Itiro Tani. “Low-speed flows involving bubble separations”. In: *Progress in Aerospace Sciences* 5 (1964), pp. 70–103.
- [27] Connor Toppings and Serhiy Yarusevych. “Linear stability analysis of a three-dimensional laminar separation bubble on a finite wing”. In: *International Journal of Heat and Fluid Flow* 101 (2023), p. 109141.
- [28] Connor Toppings and Serhiy Yarusevych. “Transient dynamics of laminar separation bubble formation and bursting”. In: *Experiments in Fluids* 64.3 (2023), p. 57.
- [29] J Verdoya et al. “Inspection of structures interaction in laminar separation bubbles with extended proper orthogonal decomposition applied to multi-plane particle image velocimetry data”. In: *Physics of Fluids* 33.4 (2021), p. 043607.
- [30] Tso-Kang Wang and Kourosh Shoele. “Kernel mode decomposition for time-frequency localization of transient flow: The formation of a laminar separation bubble”. In: *Physical Review Fluids* 8.6 (2023), p. 064401.
- [31] Julien Weiss et al. “Spectral proper orthogonal decomposition of unsteady wall shear stress under a turbulent separation bubble”. In: *AIAA Journal* 60.4 (2022), pp. 2150–2159.
- [32] Wen Wu, Charles Meneveau, and Rajat Mittal. “Spatio-temporal dynamics of turbulent separation bubbles”. In: *Journal of Fluid Mechanics* 883 (2020).
- [33] Changliang Ye et al. “Investigation on transition characteristics of laminar separation bubble on a hydrofoil”. In: *Physics of Fluids* 35.10 (2023).